Rev.Adv.Mater.Sci. 26(2010) 91-97

NUCLEATION OF NANOSCALE VOIDS AT DISCLINATION QUADRUPOLES IN DEFORMED NANOCRYSTALLINE MATERIALS

D.A. Indeitsev, N.F. Morozov, I.A. Ovid'ko and N.V. Skiba

Institute of Problems of Mechanical Engineering, Russian Academy of Sciences, Bolshoj 61, Vasil. Ostrov, St. Petersburg 199178, Russia

Received: October 3, 2010

Abstract. A special micromechanism for formation of nanoscale voids in deformed nanocrystalline materials is suggested and theoretically described. Within our description, the nanovoid nucleation represents a process driven by release of the elastic energy of disclination quadrupoles formed due to grain boundary splitting and migration. It is shown that the nanovoid nucleation at disclination quadrupoles occurs as an energetically favorable process in deformed nanocrystalline α-Al_2O_3 (sapphire), Si (silicon), and Ni (nickel) in wide ranges of their parameters.

1.INTRODUCTION

The mechanical properties of solids are crucially influenced by generation and evolution of defects; see, e.g., [1-10]. In particular, deformation-induced formation of voids at grain boundaries (GBs) and their triple junctions shows significant effects on mechanical properties of microcrystalline, ultrafine-grained and nanocrystalline materials at various plastic and superplastic deformation regimes [11-13]. For instance, voids serve as nuclei of ductile dimples at fracture surfaces or, more generally, carriers of ductile fracture processes [14,15]. Also, voids can stop propagation of brittle sharp cracks (when a sharp crack tip reaches a void and thereby becomes blunt), in which case their presence in a deformed specimen enhances its ductility. At the same time, voids cause external stress concentration [16,17] and thus contribute to decrease in ductility. Besides, nanoscale voids strongly influence the elastic properties of solids [18,19].

With the effects of voids on the deformation behavior of solids, of particular interest are fundamental micromechanisms for their deformation-induced formation in solids. In microcrystalline and ultrafine-grained materials at superplastic deformation, deformation-induced formation of voids is treated to occur as a local process releasing high local stresses created by either GB dislocation pile-ups stopped at triple junctions and ledges of GBs [11,12,20] or lattice dislocation pile-ups stopped at GBs [11,13]. When the grain size of a material decreases down to the nanometer scale, pile-ups of GB and lattice dislocations cease to be formed due to evident geometric restrictions. In this context, one expects that specific micromechanisms (different from those operating in coarse-grained polycrystals and ultrafine-grained materials) for deformation-induced formation of voids come into play in nanocrystalline materials with finest grains. This view is based on the fact [21-23] that, in parallel with conventional lattice dislocation slip, specific deformation modes effectively operate in nanocrystalline materials with finest grains. Among such deformation modes, there are GB sliding [21-23] as well as stress-driven GB migration [22,24-30] which may be accompanied by splitting of GBs and formation

Corresponding author: I.A. Ovid'ko, email: ovidko@nano.ipme.com

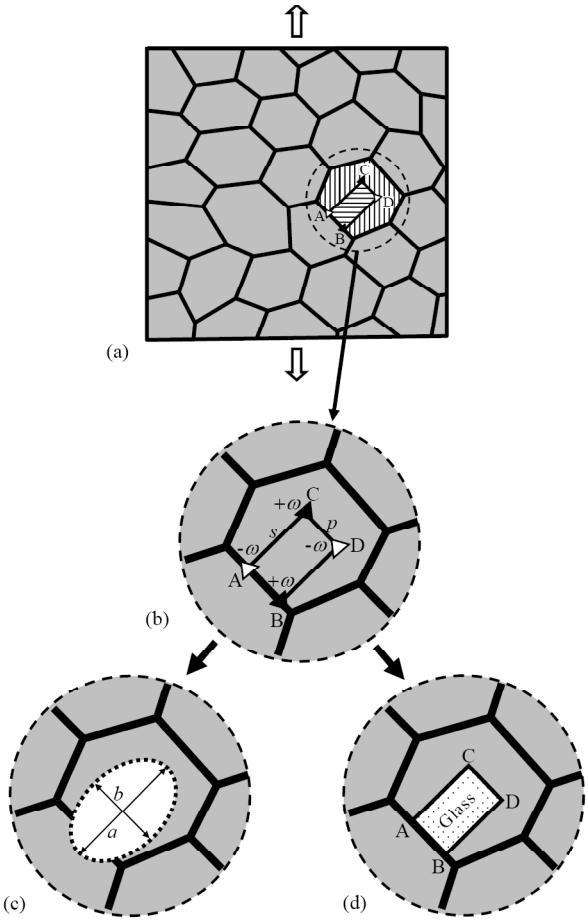

Fig. 1. Formation of a nanoscale elliptic void and a nanoscale amorphous region at a disclination quadrupole in nanocrystalline specimen deformed by stress-driven splitting and migration of grain boundaries. (a) General view. (b) Stress-driven splitting of a high-angle tilt boundary into immobile tilt boundary AB and mobile tilt boundary that migrates towards the position CD. The cooperative process in question results in formation of the new nanograin ABCD. Also, a quadrupole of wedge disclinations A, B, C, and D (with disclination strengths $\pm\omega$ and the distances *s* and *p* between the wedge disclinations) is generated in a nanocrystalline specimen due to grain boundary splitting and migration. (c) A nanoscale elliptic void (with the axes *a* and *b*) forms which absorbs the disclination quadrupole. (d) A nanoscale amorphous region nucleates at the disclination quadrupole.

of new nanograins [31,32]. GB sliding produces GB disclination dipoles [33,34], while stress-driven GB migration and nanograin formation produce GB disclination quadrupoles [28-32,35] in nanocrystalline materials. These disclination configurations create high stresses in local regions of a solid [28-35], and formation of nanovoids can serve as a process releasing the stresses. Recently, a theoretical model has been suggested describing formation of nanovoids at GB disclination dipoles in nanocrystalline materials [15]. We think that a similar nanovoid nucleation process can occur at GB disclination quadrupoles as well (Figs. 1a-1c). The main aim of this paper is to theoretically describe formation of nanoscale voids at GB disclination quadrupoles (Figs. 1a-1c) in nanocrystalline materials, examine its energy characteristics and compare them with those for formation of nanoscale amorphous regions at disclination quadrupoles (Fig. 1d).

2. FORMATION OF NANOSCALE VOIDS AT DISCLINATION QUADRUPOLES. GENERAL ASPECTS

Let us consider a nanocrystalline solid consisting of nanoscale grains divided by GBs. The solid is under a remote tensile load. A two-dimensional sec-

tion of the solid is schematically shown in Fig. 1a. We examine the situation where stress-driven GB migration contributes to plastic flow of the nanocrystalline solid (Figs. 1a and 1b). Such a situation is rather typical during plastic deformation of nanocrystalline materials [22,24-28]. Sometimes, splitting and migration of GBs occur cooperatively and result in formation of a new nanograin (Figs. 1a and 1b). Hereinafter, for definiteness, we will focus our examination to the namely situation with nucleation of a new nanograin through splitting and migration of GBs (Figs. 1a and 1b).

Following [28-32,35], GB disclination quadrupoles typically form due to stress-driven GB migration. For instance, Fig. 1b schematically shows the stress-driven splitting of a high-angle tilt boundary into immobile tilt boundary AB and mobile tilt boundary that migrates towards the position CD. The cooperative process in question results in formation of the new nanograin ABCD (Figs. 1a and 1b). Also, the angle gap ω appears at the GB junctions A and D, and the angle gap $-\omega$ appears at the GB junctions B and C (Fig. 1b), where ω is the tilt misorientation of the migrating boundary; for details, see [28-32,35]. In the theory of defects in solids, the junctions A, B, C, and D with the angle gaps $\pm\omega$ represent wedge disclinations which are characterized by the strengths $\pm\omega$ [36,37] and form a quadrudipole configuration. Hereinafter we consider a GB disclination quadrupole ABCD characterized by both the disclination strengths $\pm\omega$ and arms (the distances between disclinations) *p* and *s* (Fig. 1b).

By analogy with microtube formation at dislocations in semiconductors [38,39] and nanovoid formation at disclination dipoles in nanocrystalline materials [15], we think that one of the channels for relaxation of stresses created by the disclination quadrupole is formation of nanovoid, as shown in Fig. 1c. More precisely, disclination quadrupoles create high stresses in their vicinity. The stress relaxation can effectively occur through nucleation of a nanovoid that "absorbs" both the disclinations and the highly stressed region in their vicinity, as it is schematically shown in Fig. 1c. In doing so, as with the nanovoid formation in thin films [40] and at disclination dipoles in nanocrystalline materials [15], the nanovoid nucleation at a disclination quadrupole represents a slow process occurring through migration of vacancies towards the highly stressed region where their coagulation produces the nanovoid.

3. ENERGY CHARACTERISTICS OF FORMATION OF NANOSCALE VOIDS AT DISCLINATION QUADRUPOLES

Let us examine the energy characteristics of the nucleation of a nanovoid at a disclination quadrupole (Fig. 1). For simplicity, we consider a two-dimensional section of a nanocrystalline solid whose structure is constant along the direction perpendicular to the section. (This two-dimensional picture effectively describes the nucleation of nanovoids in nanocrystalline films and serves as a first approximation model for the same process in bulk nanocrystalline materials.) Within our approach, the nanovoid in a two-dimensional section of the solid represents an ellipse with sixes, *a* and *b*, of its axes (Fig. 1). The ellipse sizes *a* and *b* are chosen from the conditions that (i) the nanovoid absorbs completely the disclination quadrupole and its vicinity; and (ii) the ellipse perimeter is minimum at given sizes, *s* and *p*, of the disclination quadrupole. Based on the conditions, we take $a = kp\sqrt{2}$ and $b = ks\sqrt{2}$, where the non-dimensional parameter $k = 1.1$.

The nucleation of the nanovoid is energetically favorable, if the energy change $\Delta W = W_2 - W_1 < 0$. Here W_1 is the energy of the initial (void-free) state with the disclination quadrupole (Fig. 1a), and W_2 is the energy of the final state containing a nanovoid (Fig. 1b). The energy change ΔW (per unit length of a disclination or, in other terms, per unit length of the nanovoid in the three-dimensional solid) can be represented as the sum of the three terms:

$$\Delta W = W_s - W_{self}^{\Delta} - W_{gb}, \qquad (1)$$

where W_s is the free surface energy of the elliptical nanovoid, W_{self}^{Δ} is the proper energy of the disclination quadrupole absorbed by the newly formed nanovoid, and W_{gb} is the energy of the GBs of the nanograin ABCD that disappears due to the nanovoid formation.

The free surface energy W_s of the elliptical nanovoid per its unit length can be written as follows:

$$W_s = 2a\gamma_s E\left(1-\frac{b^2}{a^2}\right), \qquad (2)$$

where γ_s is the specific (per unit area) energy of the free surface, and $E(m) = \int_0^{\pi/2}\left(1 - m\sin^2\theta\right)^{1/2} d\theta$ is the complete elliptic integral of the second kind.

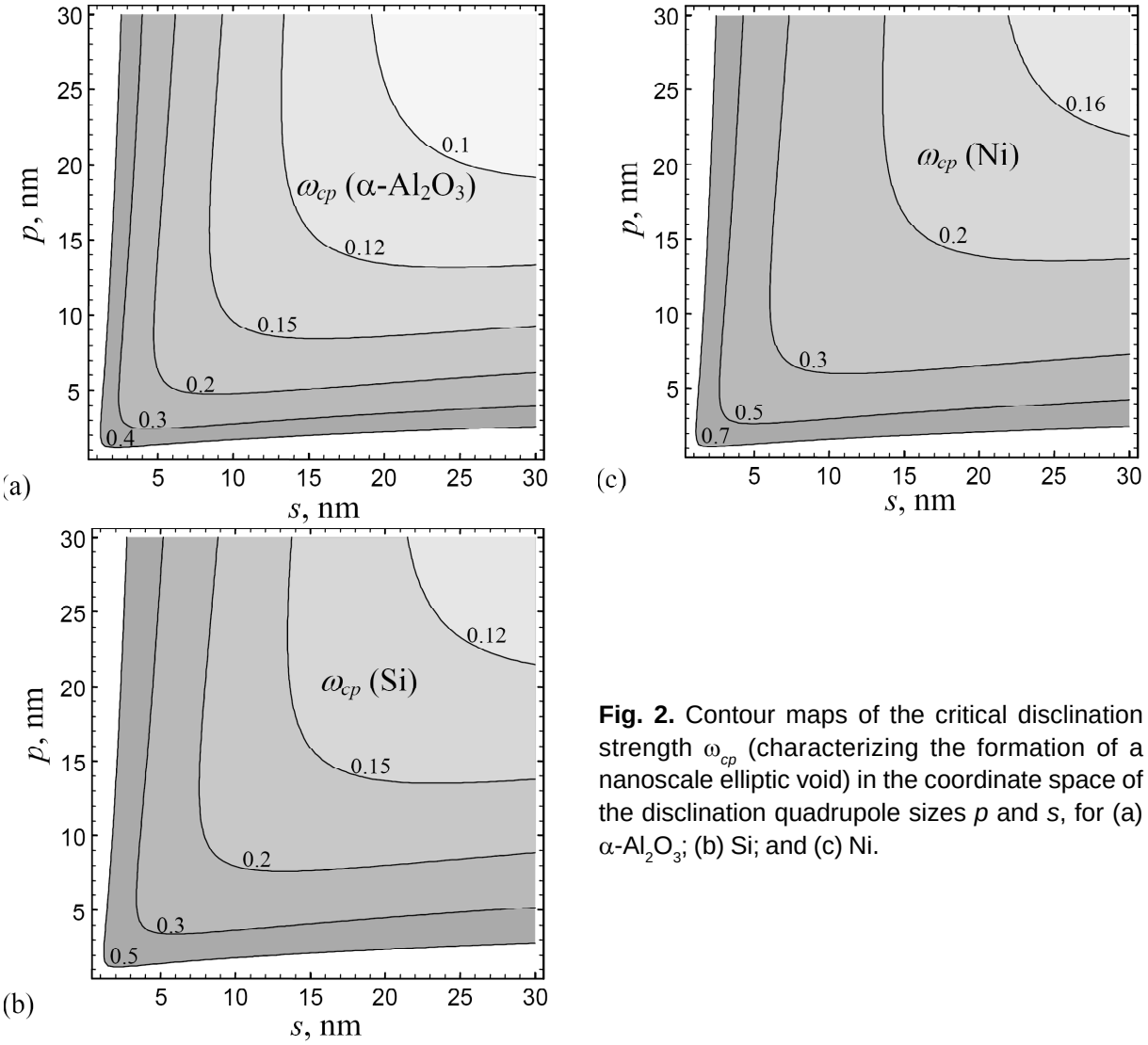

Fig. 2. Contour maps of the critical disclination strength ω_{cp} (characterizing the formation of a nanoscale elliptic void) in the coordinate space of the disclination quadrupole sizes p and s, for (a) α-Al_2O_3; (b) Si; and (c) Ni.

The proper energy W_{self}^{Δ} of the disclination quadrupole in an infinite isotropic solid is given by the standard expression [41]:

$$W_{self}^{\Delta} = \frac{D\omega^2 p^2}{2}\left(\left(1+t^2\right)\ln\left[1+t^2\right]-t^2\ln t^2\right), \qquad (3)$$

where $t = s/p$, $D = G/[2\pi(1 - \nu)]$. The energy W_{gb} of the absorbed GBs (with lengths s and p) of the rectangular nanograin ABCD is evidently given as:

$$W_{gb} \approx 2\left(s+p\right)\gamma_{gb}, \qquad (4)$$

where γ_{gb} is the specific (per unit area) GB energy.

Formulas (1)-(4) allow one to calculate the energy change ΔW. In the scientifically and technologically interesting cases of nanocrystalline ceramic α-Al_2O_3 (sapphire), nanocrystalline Si and Ni, we calculated ΔW. In doing so, we used the following typical values of parameters of α-Al_2O_3 [42]: G = 169 GPa, ν = 0.23 [42], γ_s = 1.5 J/m^2, γ_{gb} = 0.5 J/m^2 [43]; the following typical values of parameters of Si: G = 68.1 GPa, ν = 0.218 [44], γ_s = 1.5 J/m^2, γ_{gb} = 1 J/m^2 [45]; and the following typical values of parameters of Ni: G = 73 GPa, ν = 0.34, γ_s = 2.28 J/m^2, γ_{gb} = 0.866 J/m^2 [44]. Our calculations have shown that there are intervals of parameters, corresponding to the energetically favorable formation of an elliptic nanovoid at the disclination quadrupole ($\Delta W < 0$) in nanocrystalline α-Al_2O_3, Si, and Ni. From the equation $\Delta W = 0$ one finds a critical value ω_{cp} of the disclination strength ω characterizing the quadrupole. In this case, ω_{cp} is defined as the minimum value of the disclination strength, at which the nanovoid generation at the disclination quadrupole is energetically favorable. We calculated the dependence of the critical disclination strength ω_{cp} on the

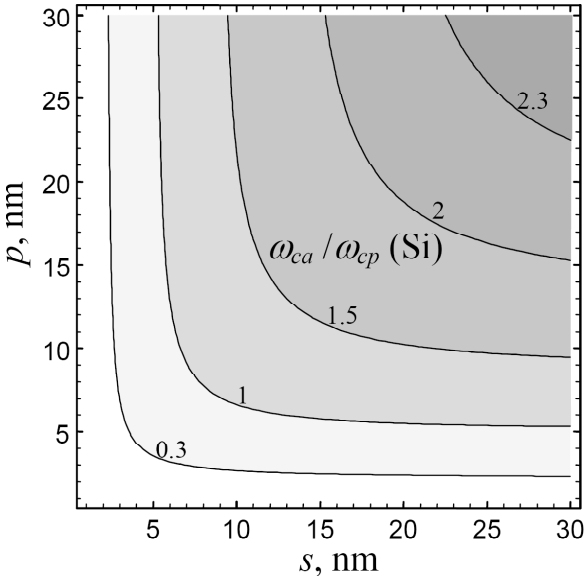

Fig. 3. Contour map of the ratio ω_{ca}/ω_{cp} in the coordinate space of the disclination quadrupole sizes *p* and *s* (for details, see text).

disclination quadrupole sizes *p* and *s* (Fig. 2). As it follows from Fig. 2, the most effective stress relation through the nanovoid formation at a disclination quadrupole – or in other terms, the lowest value of the critical disclination strength ω_{cp} – corresponds to the square-like shape (*p* = *s*) of the newly formed nanograin ABCD. That is, the nanovoid formation is enhanced at square nanograins (or those having the shape close to square), compared to the nanovoid formation at elongated nanograins. Also, as it follows from Fig. 2, the nanovoid formation is enhanced when the quadrupole sizes *p* and *s* increase.

4. COMPETITION BETWEEN FORMATION OF NANOSCALE VOIDS AND NANOSCALE AMORPHIZATION AT DISCLINATION QUADRUPOLES IN NANOCRYSTALLINE SILICON

In parallel with the nanovoid formation processes, there are alternative ways for relaxation of the local stresses created by GB disclination quadrupoles. One of such ways is the formation of nanoscale amorphous regions (nanoamorphization) at disclination quadrupoles (Fig. 1d) [46]. In general, the amorphous phase has the structure and mechanical properties significantly different from those of the crystalline phase (see, e.g., [47-54]), and formation of nanoscale amorphous regions dramatically changes the deformation behavior of a solid. In this context, it is interesting to compare the conditions for the nanovoid formation and those for nanoamorphization at GB disclination quadrupoles.

Following Ref. [46], nanoamorphization at GB disclination quadrupoles (formed during deformation-induced nucleation of nanograins; Fig 1 d) is characterized by the critical disclination strength ω_{ca} of the quadrupole, that is, the minimum disclination strength at which the energetically favorable nanoamorphization at the disclination quadrupoles occurs. With both the dependences presented in Fig. 2 and results of paper [46], we compared the critical disclination strength ω_{cp} characterizing the nanovoid formation and the critical disclination strength ω_{ca} (given by formula (5) in paper [46]). The dependence of ratio ω_{ca}/ω_{cp} on the disclination quadrupole sizes *p* and *s* is presented in Fig. 3. As it follows from Fig. 3, when the size *p* is small and/or the size *s* is small, the amorphization at a disclination quadrupole is more energetically favorable than the nanovoid formation in silicon.

5. CONCLUDING REMARKS

Thus, following the results of our theoretical analysis, the generation of nanovoids at disclination quadrupoles (Figs. 1a-1c) can effectively occur as an energetically favorable process driven by stress relaxation in deformed nanocrystalline materials. Such nanovoids slowly nucleate in the stress fields of GB disclination quadrupoles formed at GB junctions due to nanograin nucleation. According to our estimates (Fig. 2), the nanovoid formation is enhanced at square nanograins (or those having the shape close to square), compared to the nanovoid formation at elongated nanograins in nanocrystalline α-Al_2O_3, Si, and Ni. In the case of nanocrystalline Si, it is found that the nanoscale amorphization at a disclination quadrupole (Fig. 1d) is more energetically favorable than the nanovoid formation (Fig. 1c) at the starting stage of nanograin growth (when the quadrupole size *p* is small and/or the quadrupole size *s* is small).

Our theoretical model accounts for experimental observation [55-57] of nanovoids at GBs in deformed nanocrystalline metals (Ni and Au). In the framework of the model, intense local plastic flow results in nanograin nucleation which precedes the nanovoid formation. The nanovoid formation is a slow, diffusion-controlled process. Deformation-induced nanovoids (Fig. 1c) can serve as nuclei for viscous dimple rupture structures experimentally observed

[58-63] at fracture surfaces of nanocrystalline materials.

Finally, note that large pile-ups of lattice dislocations – stress sources that often induce the generation of voids and brittle cracks in conventional coarse-grained polycrystals – are hardly formed in nanoscale grains of deformed nanocrystalline materials [23,31,32]. Therefore, the formation of nanovoids at GB disclination quadrupoles (Fig. 1c), as with the formation of nanovoids at GB disclination quadrupoles [15], can play the role of the dominant fracture process at the nanoscale level in nanocrystalline materials showing ductile fracture behavior.

ACKNOWLEDGEMENTS

The work was supported, in part, by the Russian Ministry of Science and Education (Contract 14.740.11.0353 and grant NSh-3776.2010.1), the Russian Academy of Sciences Program "Fundamental studies in nanotechnologies and nanomaterials", and the Russian Foundation of Basic Research (grant 08-01-00225-a).

REFERENCES

[1] R.B. Figueiredo, M. Kawasaki and T.G. Langdon // *Rev. Adv. Mater. Sci*. **19** (2009) 1.
[2] G.J. Weng // *Rev. Adv. Mater. Sci*. **19** (2009) 41.
[3] R.A. Andrievski // *Rev. Adv. Mater. Sci.* **21** (2009) 107.
[4] E.D. Tabachnikova, V.Z. Bengus, A.V. Podolskiy, S.N. Smirnov, K. Csach, J. Miskuf, L.R. Saitova, I.P. Semenova and R.Z. Valiev // *Rev. Adv. Mater. Sci.* **18** (2008) 604.
[5] R.A. Andrievski // *Rev. Adv. Mater. Sci.* **22** (2009) 1.
[6] S.V. Bobylev, A.K. Mukherjee and I.A. Ovid'ko // *Rev. Adv. Mater. Sci.* **19** (2009)103.
[7] T. Yamasaki, H. Yokoyama and T. Fukami // *Rev. Adv. Mater. Sci.* **18** (2008) 711.
[8] S.V. Bobylev, A.K. Mukherjee, I.A. Ovid'ko and A.G. Sheinerman // *Rev. Adv. Mater. Sci.* **21** (2009) 99.
[9] M.Yu. Gutkin and I.A. Ovid'ko // *Rev. Adv. Mater. Sci.* **21** (2009) 139.
[10] S.V. Bobylev and I.A. Ovid'ko // *Rev. Adv. Mater. Sci.* **22** (2009) 39.
[11] Gouthama and K.A. Padmanabhan // *Scr. Mater.* **49** (2003) 761.
[12] A.H. Chokshi // *Mater. Sci. Eng. A* **410-411** (2005) 93.
[13] R.W. Armstrong // *Rev. Adv. Mater. Sci.* **19** (2009) 13.
[14] H. Iwasaki, K. Higashi and T.G. Nieh // *Scr. Mater.* **50** (2004) 395.
[15] I.A. Ovid'ko, A.G. Sheinerman and N.V. Skiba // *Acta Mater*. **59** (2011) 688.
[16] L.H. He and Z.R. Li // *Int. J. Solids and Structures* **43** 20 (2006) 6208.
[17] Z.R. Li, C.W. Lim and L.H. He // *Eur. J. Mech. A/Solids* **25** (2006) 260.
[18] H.L. Duan, J. Wang, Z.P. Huang and B.L. Karihaloo // *J. Mech. Phys. Sol*. **53** (2005) 1574.
[19] H.L. Duan, J. Wang, B.L. Karihaloo and Z.P. Huang // *Acta Mater*. **54** (2006) 1574.
[20] I.A. Ovid'ko and A.G. Sheinerman // *Phil. Mag*. **86** (2006) 3487.
[21] K.S. Kumar, S. Suresh and H. Van Swygenhoven // *Acta Mater*. **51** (2003) 5743.
[22] M. Dao, L. Lu, R.J. Asaro, J.T.M. De Hosson and E. Ma // *Acta Mater.* **55** (2007) 4041.
[23] C.C. Koch, I.A. Ovid'ko, S. Seal and S. Veprek, *Structural Nanocrystalline Materials: Fundamentals and Applications* (Cambridge University Press, Cambridge, 2007).
[24] M. Jin, A.M. Minor, E.A. Stach and J.W. Morris Jr. // *Acta Mater*. **52** (2004) 5381.
[25] W.A. Soer, J.Th.M. De Hosson, A.M. Minor, J.W. Morris Jr. and E.A. Stach // *Acta Mater*. **52** (2004) 5783.
[26] J.T.M. De Hosson, W.A. Soer, A.M. Minor, Z. Shan, E.A. Stach, S.A. Syed Asif and O.L. Warren // *J. Mater. Sci*. **41** (2006) 7704.
[27] D.S. Gianola, D.H. Warner, J.F. Molinari and K.J. Hemker // *Scr. Mater*. **55** (2006) 649.
[28] G.J. Fan, L.F. Fu, H. Choo, P.K. Liaw and N.D. Browning // *Acta Mater*. **54** (2006) 4781.
[29] M.Yu. Gutkin and I.A. Ovid'ko // *Appl. Phys. Lett*. **87** (2005) 251916.
[30] I.A. Ovid'ko, A.G. Sheinerman and E.C. Aifantis // *Acta Mater*. **56** (2008) 2718.
[31] S.V. Bobylev and I.A. Ovid'ko ***II*** *Appl. Phys. Lett*. **92** (2008) 081914.
[32] S.V. Bobylev and I.A. Ovid'ko // *Rev. Adv. Mater. Sci.* **17** (2008) 76.
[33] S.V. Bobylev, N.F. Morozov and I.A. Ovid'ko // *Phys. Rev. Lett*. **105** (2010) 055504.
[34] N.F. Morozov, I.A. Ovidko, Yu.V. Petrov and A.G. Sheinerman // *Rev. Adv. Mater. Sci.* **19** (2009) 63.
[35] M.Yu Gutkin, K.N. Mikaelyan and I.A. Ovid'ko // *Scr. Mater*. **58** (2008) 850.

[36] M. Kleman and J. Friedel // *Rev. Mod. Phys*. **80** (2008) 61.
[37] A.E. Romanov and A.L. Kolesnikova // *Progr. Mater. Sci*. **54** (2009) 740.
[38] F.C. Frank // *Acta Cryst*. **4** (1951) 497.
[39] X. Ma // *J. Appl. Phys*. **99** (2006) 063513.
[40] A.S. Vladimirov, R.V. Goldshtein, Yu.V. Zhitnikov, M.E. Sarychev and D.B. Shirabaikin // *Mathem. Modelirovanie* **14** (2002) 95.
[41] M.Yu. Gutkin, K.N. Mikaelyan, A.E. Romanov and P. Klimanek // *Phys. Status Solidi (a)* **193** (2002) 35.
[42] R.G. Munro // *J. Am. Ceram. Soc*. **80** (1997) 1919.
[43] T. Watanabe, H. Yoshida, T. Saito, T. Yamamoto, Y. Ikuhara and T. Sakuma // *Mater. Sci. Forum* **304-306** (1999) 601.
[44] J.P. Hirth and J. Lothe, *Theory of Dislocations* (Wiley, New York, 1982).
[45] M. Kohyama // *Modell. Simul. Mater. Sci. Eng*. **10** (2002) R31.
[46] S.V. Bobylev and I.A. Ovid'ko // *Appl. Phys. Lett*. **93** (2008) 061904.
[47] A. Inoue, X.M. Wang and W. Zhang // *Rev. Adv. Mater. Sci*. **18** (2008) 1.
[48] G.Y. Wang, P.K. Liaw, A. Smyth, M. Denda, A. Peker, M. Freels, R.A. Buchanan and C.R. Brooks // *Rev. Adv. Mater. Sci.* **18** (2008) 18.
[49] K. Hajlaoui, M. Stoica, A. LeMoulec, F. Charlot and A.R. Yavari // *Rev. Adv. Mater. Sci.* **18** (2008) 23.
[50] K. Amiya and A. Inoue // *Rev. Adv. Mater. Sci*. **18** (2008) 27.
[51] P. Rizzi, M. Satta and M. Baricco // *Rev. Adv. Mater. Sci*. **18** (2008) 66.
[52] K. Fujita, T. Hashimoto, W. Zhang, N. Nishiyama, C. Ma, H. Kimura and A. Inoue // *Rev. Adv. Mater. Sci.* **18** (2008) 137.
[53] E. Pineda and D. Crespo // *Rev. Adv. Mater. Sci*. **18** (2008) 173.
[54] C. Duhamel, J. Das, S. Pauly, K.S. Lee and J. Eckert // *Rev. Adv. Mater. Sci*. **18** (2008) 527.
[55] W.W. Milligan, S.A. Hackney, M. Ke and E.C. Aifantis // *Nanostruct. Mater.* **2** (1993) 267.
[56] M. Ke, W.W. Milligan, S.A. Hackney, J.E. Carsley and E.C. Aifantis // *Nanostruct. Mater.* **5** (1995) 689.
[57] K.S. Kumar, S. Suresh, M.F. Chisholm, J.A. Horton and P. Wang // *Acta Mater*. **51** (2003) 387.
[58] H. Li and F. Ebrahimi // *Appl. Phys. Lett*. **84** (2004) 4307.
[59] H. Li and F. Ebrahimi // *Adv. Mater*. **17** (2005) 1969.
[60] K.-M. Youssef, R.O. Scattergood, K.L. Murty and C.C. Koch // *Appl. Phys. Lett*. **85** (2004) 929.
[61] S. Cheng, E. Ma, Y.M. Wang, L.J. Kecskes, K.M. Youssef, C.C. Koch, U.P. Trociewitz and K. Han // *Acta Mater.* **53** (2005) 1521.
[62] K.M. Youssef, R.O. Scattergood, K.L. Murty and C.C. Koch // *Scr. Mater*. **54** (2006) 251.
[63] F. Ebrahimi, A.J. Liscano, D. Kong, Q. Zhai and H. Li // *Rev. Adv. Mater. Sci*. **13** (2006) 33.